DYNAMICAL BEHAVIOUR OF A LINEAR MAGLEV SUPPORT UNIT FOR FAST TOOLING MACHINES

Karl-Dieter Tieste
Karl Popp
Institute of Mechanics, University of Hannover, Germany

ABSTRACT

Tooling machines with an aimed velocity to accuracy ratio of $600\frac{\mathrm{m/min}}{\mathrm{mm}}$ and higher require linear guides with high slide velocity and very high position accuracy.

To obtain these aims three tasks — supporting, guiding and actuating of a translational support unit — shall be realised by means of active magnetic bearings (AMB). The resulting linear maglev-guide for tooling machines must exhibit the following characteristics: high stiffness, good damping and low noise levels as well as low heat production.

First research on a one degree-of-freedom (DOF) support magnet unit aimed at the development of components and efficient control strategies for the linear maglev-guide. Subsequent research is directed to realise a five DOF maglev linear-guide for fast tooling machines.

This paper describes results of the one DOF support magnet unit and first results of the complete maglev linear guide.

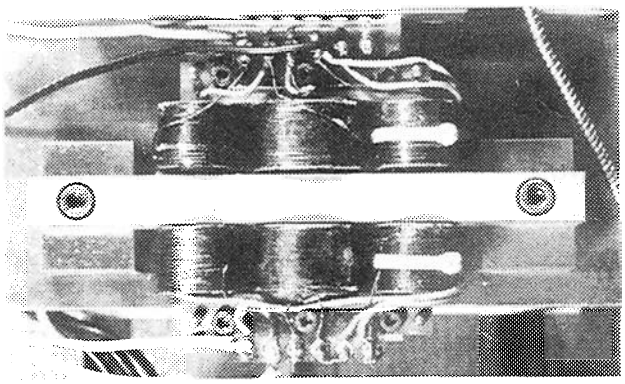

Figure 1: The 1 DOF magnetic bearing

THE ONE DOF MAGNETIC BEARING

The one DOF magnetic bearing shown in fig.1 consists of a pair of electromagnets in differential arrangement and a mass of 11kg guided by roller bearings. The characteristics of the electromagnets are: pole area: $A = 10\mathrm{cm}^2$, coil: 500 turns, $R = 1.6\Omega$, $L = 0.072\mathrm{H}$. The overall maximum static force is 650N at a nominal air gap of 0.9mm.

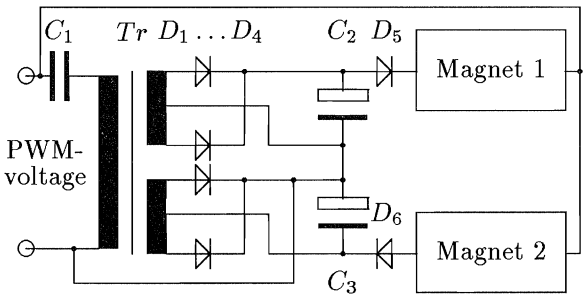

Figure 2: Premagnetisation circuit

Premagnetization

The forces of the electromagnets counteract due to the differential arrangement. A special type of premagnetisation is used in the voltage controlled AMB that is shown in fig.2. The pulse-width-modulated voltage of the power amplifier is used in a double way: the low frequency component is used for the levitation of the electromagnets. The high frequency AC component is first decoupled by the capaicitor C_1 from the DC component. The transformer Tr, in conjunction with the diodes $D_1..D_4$, and the electrolytic capacitors C_2, C_3 generates two DC voltages inducing a loop current through the electromagnets. The diodes D_5 and D_6 prevent reverse currents through the electromagnets. This kind of premag-

netisation has the advantage of high overdriveability, good linearity and low leakage power and, thus, low heat production. The force-current-relation is shown in fig.3.

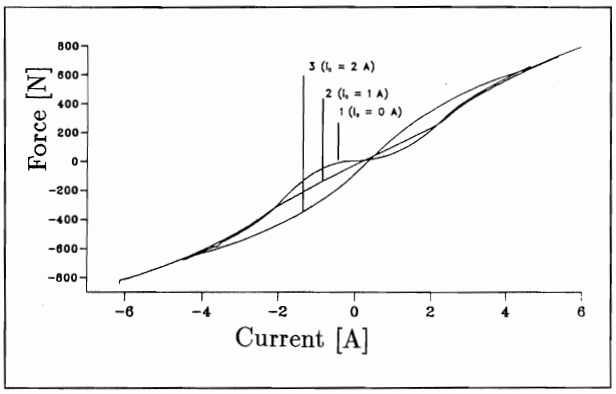

Figure 3: Force-current-relation, $I_v = 0; 1.0; 2.0A$, air gap $= x_0 = 0.9mm$

Control System

A linear model is used for the voltage controlled magnetic bearing, which is shown in fig. 4. The model consists of a linear electromagnet with the coefficients L, R, the force-current coefficient k_i, the mass m, the (negative) stiffness k_c and the induction coefficient k_v. The corrosponding set of differential equations are

$$\dot{i} = \frac{-R}{L}\, i - k_v\, \dot{x} + \frac{1}{L}\, U, \qquad (1)$$

$$\ddot{x} = \frac{1}{m}\,(k_c\, x + k_i\, i) \qquad (2)$$

which can be written in state space presentation as

$$\frac{d}{d\,t}\begin{pmatrix} x \\ \dot{x} \\ i \end{pmatrix} = \begin{pmatrix} 0 & 1 & 0 \\ \frac{k_c}{m} & 0 & \frac{k_i}{m} \\ 0 & -k_v & \frac{-R}{L} \end{pmatrix} \begin{pmatrix} x \\ \dot{x} \\ i \end{pmatrix} + \begin{pmatrix} 0 \\ 0 \\ \frac{1}{L} \end{pmatrix} U. \qquad (3)$$

The structure of the controller for the one DOF magnetic bearing is shown in fig. 5. The three state variables of the electromagnet are gained by means of an observer. The control variable is generated by state feedback of the observed states supplemented by an additional integral stage. The static accuracy of the magnetic bearing is very high because of the additional integral state in the control system. The dynamical behaviour of the magnetic bearing is defined by the location of the poles of the observer and of the controller. The feedback gains have been calculated by pole assignment. It turned out that a configuration of four equal real poles give best results.

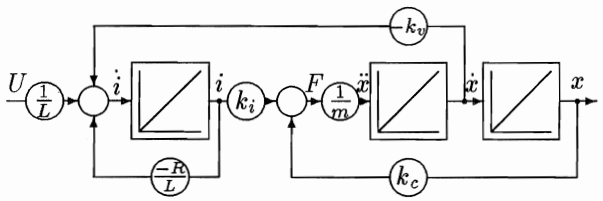

Figure 4: Model of the magnetic bearing

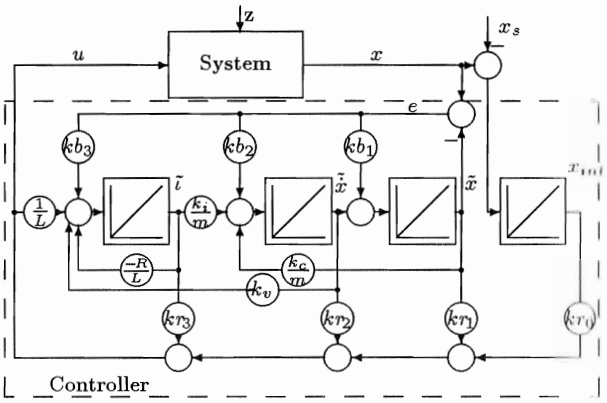

Figure 5: Electromagnet with observer and state control

Parameter Identification

The quality of the control highly depends on the degree of accurate knowledge of the magnet parameters. First, these parameters have been measured by direct measurements. However, if the controller is able to stabilize the magnetic bearing in its operating point then it is possible to identify the parameters of the electromagnet by using model-fitting procedures. For this a gaussian white noise $r(t)$ is added to the control variable causing an excitation of the AMB. An additional simulation model of the electromagnet is connected to the input and output of the controlled system. The simulation model must also be stable, thus, an error feedback like the observer feedback is necessary (cf. fig. 6). The parameters of the model are adjusted in the way that the variance of the control devitation $e = x - \tilde{x}$ of the simulated and the controlled system gets minimal,

$$J = \int_0^T e^2 \stackrel{!}{=} \text{Min.} \qquad (4)$$

Thus, the identification problem is reduced to a nonlinear optimisation problem. The minimum can be found by different strategies. First a strategy has been used with a sequential parameter search along the axes in the parameter space, but the calculation time is high. The simplex method described by NELDER and MEAD[1] works much faster. Both

identification methods are robust, resulting in parameters which give much better control results in the experiments compared to those by direct measurements of the parameters.

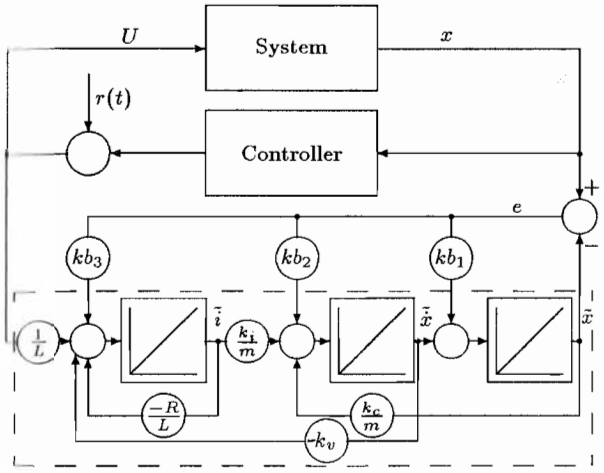

Figure 6: Parameter identification of the controlled system

Pole location

After the identification of the parameters the control gains have been optimised. The optimisation goal is to reach high stiffness, good damping and low noise levels.

There is s trade off between noise and stiffness of the AMB. High stiffness but also high noise levels are achieved by using fast control dynamics. For optimising the control gains the frequency-responses of the stiffness $\frac{X(s)}{F(s)}$ and the noise $\frac{U(s)}{X(s)}$ can be used to formulate an overall criterion, which has to be minimised by non-linear optimisation. This results in the optimum pole configuration for the given overall criterion. Again, it turns out that a configuration of equal real poles gives best results.

In fig. 7 the frequency-response of the compliance is shown. Typical tooling machines with operating lengths of 1m show a dynamical stiffness of $20\frac{N}{\mu m}$[2]. The stiffness obtained by this AMB is much less, but the damping ($D = 0.5..1$) is very high compared to typical tooling machines ($D = 0.01..0.05$).

THE MAGLEV LINEAR GUIDE

The maglev linear guide consists of a guide block with six pairs of electromagnets (two horizontal magnets and four vertical magnets) in differential arrangement and a guideway with three rails cf. fig. 8. The nomimal air gap of the guide is only 0.35 mm wide to achieve high stiffness. The characteristics

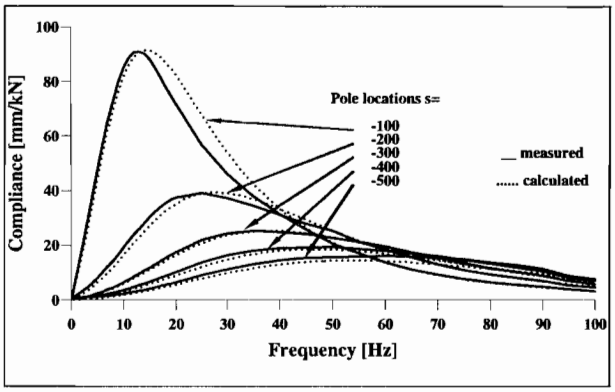

Figure 7: Frequency-response of compliance of the one DOF magnetic bearing

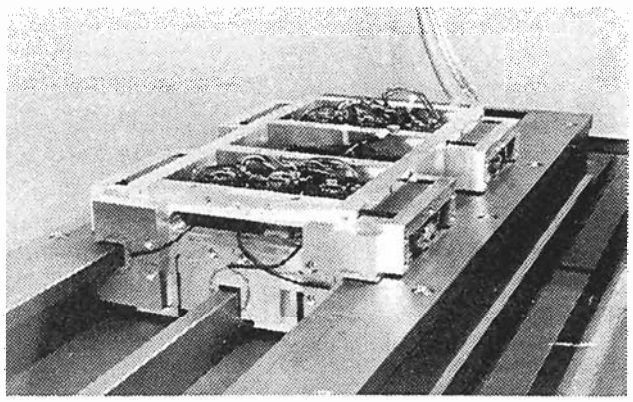

Figure 8: The maglev linear guide

of the electromagnets are: pole area: $A = 10$ cm^2, coil: 500 turns, $R = 1.9\ \Omega$, $L = 0.12$ H, $k_i = 400\ \frac{\mathrm{N}}{\mathrm{A}}$, $k_v = 3.4\ 10^3\ \frac{\mathrm{A}}{\mathrm{m}}$ and $k_c = 1.4\ 10^6\ \frac{\mathrm{N}}{\mathrm{m}}$. The mass is $m = 26.6$ kg and the moments of interia are $J_x^{(c)} = 0.24$ kg m^2, $J_y^{(c)} = 0.45$ kg m^2 and $J_z^{(c)} = 0.64$ kg m^2. The lever of the magnets are: $a = 0.03$m, $b = 0.123$m, $c = 0.125$m and the lever of the sensors are $a_s = 0.03$m, $b_s = 0.123$m, $c_s = 0.21$m. The maglev linear guide is designed for a nominal load of 2 kN.

In general two control concepts can be distinguished: i) Decentralised single-magnet control, where each magnet has its own controller and may be also its own measuring system. ii) Centralised degree-of-freedom (DOF) control, where each DOF or mode has a controller using a centralised measuring system. In the present case of a linear guide with 5 DOF and 6 electromagnets having 6 input voltages ($U_1 \ldots U_6$) and a measuring system with 6 output displacements ($x_{s1} \ldots x_{s6}$) there is no big difference in the costs of a realisation of the two concepts. However, with respect to the dynamic performance of the linear guide concept ii) is preferable.

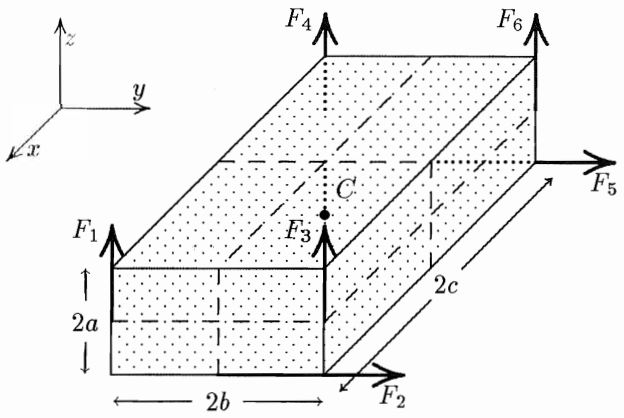

Figure 9: Coordinate system and free body diagram

Equations of Motion

The coordinate system and the free body diagram shown in fig. 9 are the basis for the equations of motion. The following simplifications have been made: All magnets are equal, the guide has no payload (at this time) so that the centre of mass C is located in the middle of the slide and the principal axes concide with the coordinate axes.

The relation between the magnet coordinates $\{x_1 \ldots x_6\}$ and the guide-coordinates $\{y, z, \varphi_x, \varphi_y, \varphi_z\}$ read:

$$y = \frac{1}{2}(x_2 + x_5) + \frac{a}{4b}(x_1 - x_3 + x_4 - x_6), \quad (5)$$

$$z = \frac{1}{4}(x_1 + x_3 + x_4 + x_6), \quad (6)$$

$$\varphi_x = \frac{1}{4b}(-x_1 + x_3 - x_4 + x_6), \quad (7)$$

$$\varphi_y = \frac{1}{4c}(-x_1 - x_3 + x_4 + x_6), \quad (8)$$

$$\varphi_z = \frac{1}{2c}(x_2 - x_5). \quad (9)$$

The differential equations for the 6 magnet currents are

$$\dot{i}_n = \frac{-R}{L} i_n - k_v \dot{x}_n + \frac{1}{L} U_n, \qquad n = 1(1)6. \quad (10)$$

The equations of motion for the two translational and the three rotational DOF are

$$\ddot{y} = \frac{1}{m}\Big(k_c(x_2 + x_5) + k_i(i_2 + i_5)\Big), \quad (11)$$

$$\ddot{z} = \frac{1}{m}\Big(k_c(x_1 + x_3 + x_4 + x_6) + k_i(i_1 + i_3 + i_4 + i_6)\Big), \quad (12)$$

$$\ddot{\varphi}_x = \frac{b}{J_x^{(c)}}\Big(k_c(-x_1 + x_3 - x_4 + x_6) + k_i(-i_1 + i_3 - i_4 + i_6)\Big) + \frac{a}{J_x^{(c)}}\Big(k_c(x_2 + x_5) + k_i(i_2 + i_5)\Big), \quad (13)$$

$$\ddot{\varphi}_y = \frac{c}{J_y^{(c)}}\Big(k_c(-x_1 - x_3 + x_4 + x_6) + k_i(-i_1 - i_3 + i_4 + i_6)\Big), \quad (14)$$

$$\ddot{\varphi}_z = \frac{c}{J_z^{(c)}}\Big(k_c(x_2 - x_5) + k_i(i_2 - i_5)\Big). \quad (15)$$

These differential equations are coupled. With the assumption $a = 0$ and by elimination of the magnet coordinates the eqs. (11) ...(15) result in

$$\ddot{y} = \frac{1}{m}\Big(2\, k_c\, y + k_i(i_2 + i_5)\Big), \quad (16)$$

$$\ddot{z} = \frac{1}{m}\Big(4\, k_c\, z + k_i(i_1 + i_3 + i_4 + i_6)\Big), \quad (17)$$

$$\ddot{\varphi}_x = \frac{b}{J_x^{(c)}}\Big(4k_c b\, \varphi_x + k_i(-i_1 + i_3 - i_4 + i_6)\Big), \quad (18)$$

$$\ddot{\varphi}_y = \frac{c}{J_y^{(c)}}\Big(4k_c c\, \varphi_y + k_i(-i_1 - i_3 + i_4 + i_6)\Big), \quad (19)$$

$$\ddot{\varphi}_z = \frac{c}{J_z^{(c)}}\Big(2k_c\, c\, \varphi_z + k_i(i_2 - i_5)\Big). \quad (20)$$

Decoupling

The sum of the currents $i_2 + i_5$ have an effect on the acceleration in y-direction only. By replacing this sum by

$$i_y = i_2 + i_5 \quad (21)$$

eq. (16) reads

$$\ddot{y} = \frac{1}{m}\Big(2\, k_c\, y + k_i\, i_y\Big). \quad (22)$$

In an analogous way the eqs. (17) ...(20) can be rewritten by replacing the currents using $i_z = i_1 + i_3 + i_4 + i_6$, $i_{\varphi_x} = -i_1 + i_3 - i_4 + i_6$, $i_{\varphi_y} = -i_1 - i_3 + i_4 + i_6$ and $i_{\varphi_z} = i_2 - i_5$. The resulting equations only depend on the coordinates of the guide and the five virtual currents $\{i_y, i_z, i_{\varphi_x}, i_{\varphi_y}$ and $i_{\varphi_x}\}$.

$$\ddot{z} = \frac{1}{m}\Big(4\, k_c\, z + k_i\, i_z\Big), \quad (23)$$

$$\ddot{\varphi}_x = \frac{b}{J_x^{(c)}}\Big(4b\, k_c\, \varphi_x + k_i\, i_{\varphi_x}\Big), \quad (24)$$

$$\ddot{\varphi}_y = \frac{c}{J_y^{(c)}}\Big(k_c 4\, c\, \varphi_y + k_i\, i_{\varphi_y}\Big), \quad (25)$$

$$\ddot{\varphi}_z = \frac{c}{J_z^{(c)}}\Big(k_c 2\, c\, \varphi_z + k_i\, i_{\varphi_z}\Big). \quad (26)$$

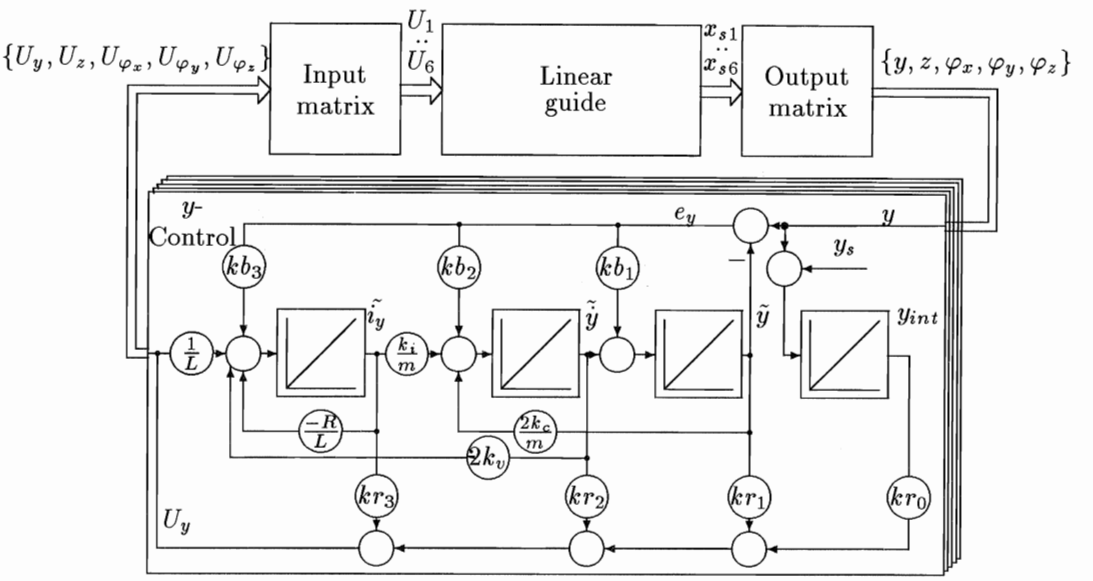

Figure 10: The control system of the maglev linear guide

The combination of the currents to the five virtual currents $\{i_y, i_z, i_{\varphi x}, i_{\varphi y}, i_{\varphi z}\}$ can be extended to an analogous combination of the voltages $\{U_y, U_z, U_{\varphi x}, U_{\varphi y}, U_{\varphi z}\}$ because of equal time-constants $\frac{-R}{L}$ of the electromagnets resulting in decoupled equations of motion with the same structure as five virtual *independent* 1 DOF magnetic bearings

$$\dot{i}_y = \frac{-R}{L} i_y - 2k_v\, \dot{y} + \frac{1}{L} U_y, \tag{27}$$

$$\ddot{y} = \frac{1}{m}\left(2\, k_c\, y + k_i\, i_y\right), \tag{28}$$

$$\dot{i}_z = \frac{-R}{L} i_z - 4\, k_v\, \dot{z} + \frac{1}{L} U_z, \tag{29}$$

$$\ddot{z} = \frac{1}{m}\left(4\, k_c\, z + k_i\, i_z\right), \tag{30}$$

$$\dot{i}_{\varphi_x} = \frac{-R}{L} i_{\varphi_x} - 4b\, k_v\, \dot{\varphi_x} + \frac{1}{L} U_{\varphi_x}, \tag{31}$$

$$\ddot{\varphi}_x = \frac{b}{J_x^{(c)}}\left(4b\, k_c\, \varphi_x + k_i\, i_{\varphi_x}\right), \tag{32}$$

$$\dot{i}_{\varphi_y} = \frac{-R}{L} i_{\varphi_y} - 4c\, k_v\, \dot{\varphi_y} + \frac{1}{L} U_{\varphi_y}, \tag{33}$$

$$\ddot{\varphi}_y = \frac{c}{J_y^{(c)}}\left(k_c 4\, c\, \varphi_y + k_i\, i_{\varphi_y}\right), \tag{34}$$

$$\dot{i}_{\varphi_z} = \frac{-R}{L} i_{\varphi_z} - 2c\, k_v\, \dot{\varphi_z} + \frac{1}{L} U_{\varphi_z}, \tag{35}$$

$$\ddot{\varphi}_z = \frac{c}{J_z^{(c)}}\left(k_c 2\, c\, \varphi_z + k_i\, i_{\varphi_z}\right). \tag{36}$$

Control System

These decoupled virtual magnetic bearings can be controlled in an analogous way as the 1 DOF magnetic bearing shown in the first part of the paper. The input equations $U_1 = U_z - U_{\varphi_x} - U_{\varphi_y}$, $U_2 = U_y + U_{\varphi_z} + \frac{a}{b} U_{\varphi_x}$, $U_3 = U_z + U_{\varphi_x} - U_{\varphi_y}$, $U_4 = U_z - U_{\varphi_x} + U_{\varphi_y}$, $U_5 = U_y - U_{\varphi_z} + \frac{a}{b} U_{\varphi_x}$ and $U_6 = U_z + U_{\varphi_x} + U_{\varphi_y}$ can be used to transform the virtual voltages of the decoupled controllers to those of the real magnets. The structure of the system shown in fig. 10 is similar to the one DOF magnetic bearing (cf. fig.5 so that the controller of the one DOF magnetic bearing can directly be used.
In this way it is possible to optimise e.g. the stiffness seperately for each DOF in a simple way.

First Results

First simulations have been made for the decoupled system. In fig.11 frequency-responses are shown of the compliance in z- and y-direction for a force acting in the centre of mass in z- and y-direction, respectively. Both frequency responses are similar but the force in y direction effects a rotation in φ_x-direction because of the distance $a \neq 0$. This coupling between the y- and the φ_x-mode leads to an distortion in the $Z - Z$-compliance at about 80Hz, cp. fig.11 and fig.12.

Further Research

Further research will be directed to realise the control of the maglev linear guide and to verify the quality of the control by experiments. Furthermore, the control system for the maglev linear guide shall be extended to comprise different payloads and corresponding positions of the center of mass.

Literature

[1] Schwefel,H.-P.: *Numerische Optimierung von Computer-Modellen mittels der Evolutionsstrategie,* Birkhäuser Verlag, Basel, Stuttgart 1977

[2] Weck, M.: *Werkzeugmaschinen, Fertigungssysteme Band 4, Messtechnische Unteruchung und Beurteilung,* VDI Verlag, Düsseldorf 1992

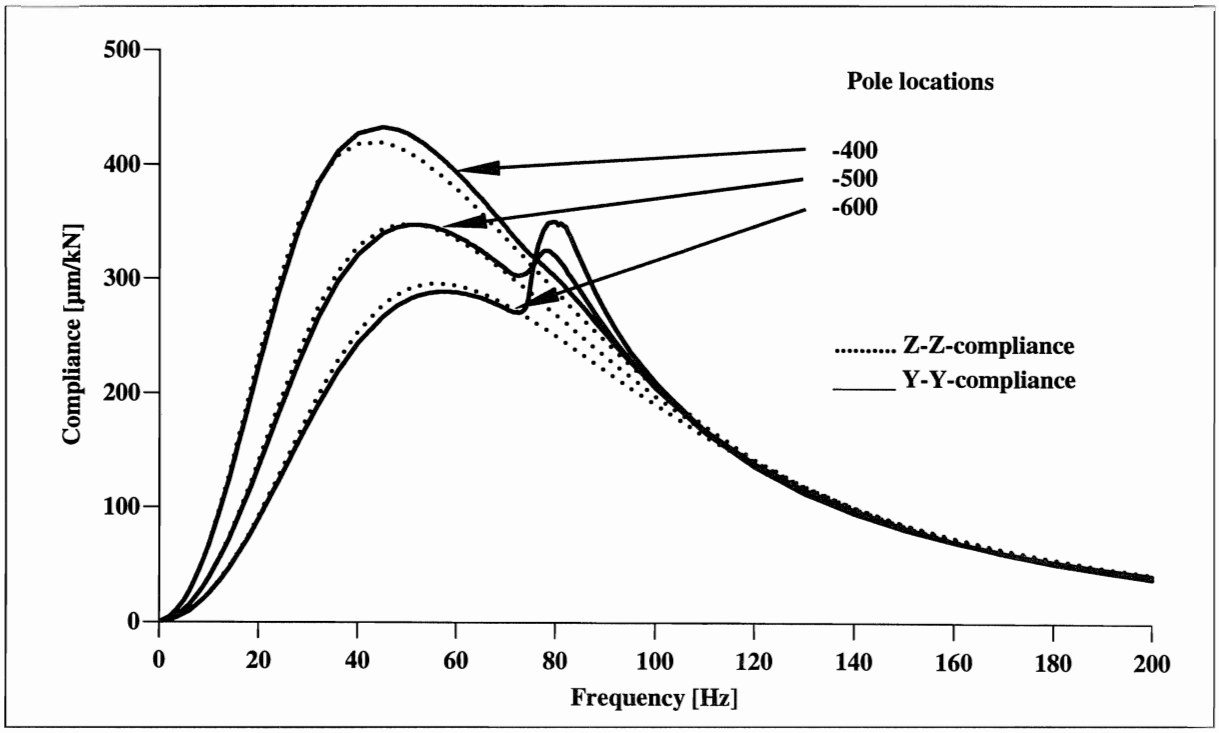

Figure 11: Frequency-response of the compliance in z- and y-direction for a force acting in the centre of mass in z- and y-direction

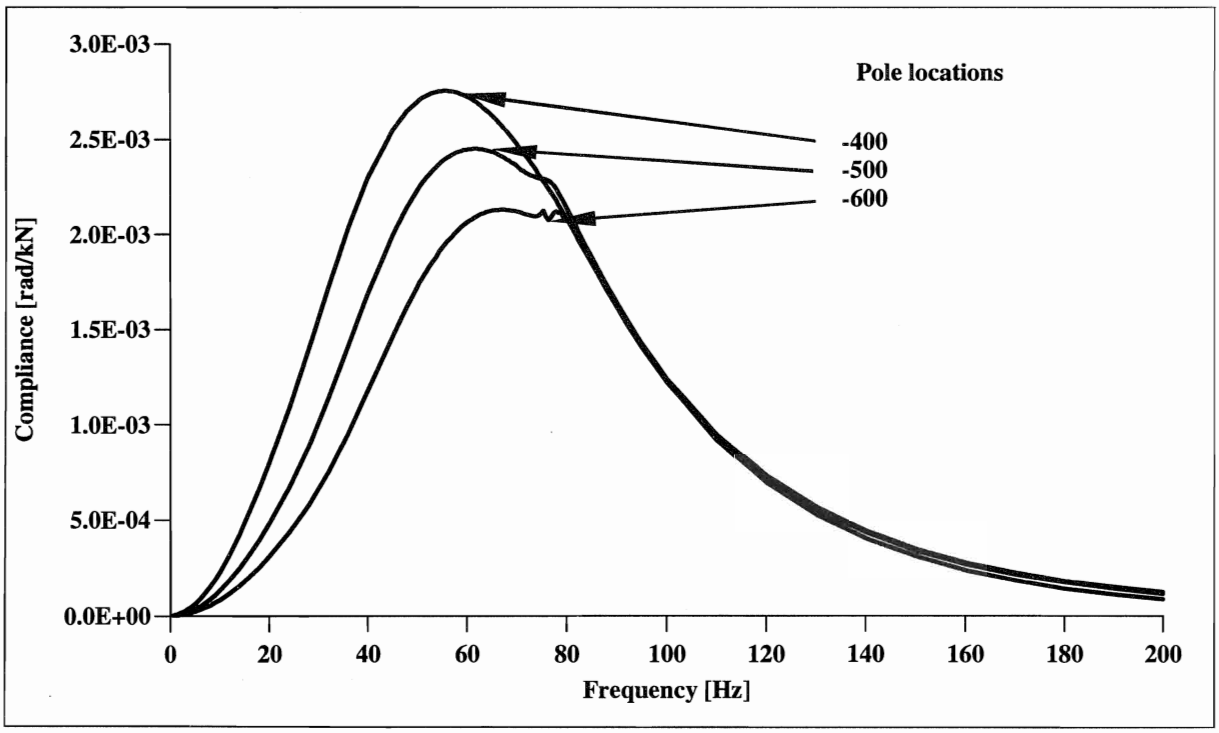

Figure 12: Frequency-response of the compliance in φ_x-direction for a force acting in the centre of mass in y-direction